Inversion of interfacial waves for the geotechnical characterisation of marine sediments in shallow water

C. Strobbia[1], A. Godio[2] and G. De Bacco[2]

[1] *European Centre for Training and Research in Earthquake Engineering, Pavia, Italy*
[2] *Dip. Ing. del Territorio, dell'Ambiente e delle Geotecnologie, Politecnico di Torino, Italy*

(Received August 5, 2005; accepted December 21, 2005)

ABSTRACT The diagnostic capability of Scholte and guided wave analysis for estimating the mechanical properties of shallow sediments is considered. The modelling of a theoretical response in 1D conditions and sensitivity analysis permit the assessment of the reliability of the approach; experimental data have been acquired in two test sites using hydrophones disposed on the sea bottom. The sites are characterised by a reduced thickness of sediments (less than 4 meters) in shallow water (2 to 15 meters) with a hard calcareous bedrock. To avoid or reduce some ambiguities in data processing, we integrate the seismic data with information derived from electrical resistivity tomography acquired using electrodes on the seabottom.

1. Introduction

The determination of seismic wave velocities (P and S wave velocity) in the first meters of marine sediments close to the shoreline can provide useful information for the site characterisation in shallow water.

Geophysical techniques allow the characterisation of large volumes of soil, in undisturbed conditions, at a very small strain: the dynamic properties provided by the seismic methods, besides being essential for seismic site response assessment, can be used to estimate physical properties, such as porosity, and to correlate with technical parameters useful for foundation designs, for slope stability assessment, for liquefaction potential evaluation, for erosion potential and so on. These can be a crucial step for the design of port structures, of artificial islands, for pipeline positioning.

The traditional shallow seismic techniques, effectively applied onshore, cannot be straightforwardly used offshore, not even in very shallow water.

P-wave refraction can be successfully used to detect a hard bedrock beneath the sediments (Shtievelman, 2001), but the use of compressional waves has an intrinsic limitation: because of the high porosity of sediments and because of the saturation, the compressibility of the soft sediments is completely dominated by the pore water, and the contrast of P-wave velocity is reduced to values that are in many situations difficult to detect with conventional refraction or reflection methods.

The use of shear waves (Vs) can overcome this problem. As is well known, the shear wave velocity, that depends on the solid skeleton mechanical properties in completely saturated loose sediments, can be much lower (even 50 times lower) than the compressional wave velocity. The

wavelength is shorter, the resolution is hence higher, and the Vs variation in the first tens of meters can be one order of magnitude greater than the Vp variation, as also observed experimentally (Hamilton, 1976). Moreover, the shear wave velocity Vs is much more sensitive to the fabric of the sediment and can be used in predicting geotechnical parameters.

The acquisition of shear waves can be however, quite critical: the use of horizontal receivers and a horizontally polarized source, which is the common procedure for onshore SH reflection and refraction at a very shallow depth (Deidda and Balia, 2001), presents difficulties even in very shallow water. The water prevents the S-wave propagation, and the coupling of the receivers and of the source needed with the sea bottom, make a traditional acquisition very problematic: a possible solution is the use of specific bottom-dragged instrumentation able to generate and detect shear waves (Stoll and Bautista, 1994, Winsborrow *et al.*, 2003).

An effective alternative to the traditional approach of engineering seismics can be the analysis of interface waves: Scholte waves (Caiti *et al*., 1994; Bohlen *et al*., 2004), Love waves (Winsborrow *et al.*, 2003) and acoustic modes (Shtivelman, 2004). Like in onshore seismics, the analysis of the vertical component of the particle motion allows the identification and inversion of surface waves, in offshore seismics the shear wave velocity profile can hence be inferred inverting the dispersion relation obtained by processing the pressure wavefield associated to interfacial waves. Two useful wave phenomena are generated and can be detected and analysed in an experiment with an impulse source and pressure receivers in a liquid layer over an elastic layered half space: both Scholte waves, whose properties mainly depend on the shear wave velocity of the sub-bottom sediments, and acoustic guided waves, whose properties mainly depend on the compressional wave velocity of the sub-bottom sediments (Nicolas *et al*., 2002; Shtivelman, 2004).

In this paper, we discuss how the analysis of such waves can be a tool for the characterisation of marine sediments in very shallow water, firstly illustrating briefly the theoretical expectation for the wave propagation in shallow water, and then, describing the acquisition and the processing that can be used in a practical shallow application. We integrate the discussion by analysing the results of the Electrical Resistivity Tomography (ERT) adopted to constrain some parameters (porosity and sediment thickness) in the seismic data processing.

The experimental application has been particularly challenging because of the presence of a thin layer of very soft sediments over a hard bedrock.

2. Theoretical background

In order to analyse the properties of interfacial waves propagated at the solid-liquid interface, the wave propagation can be solved using a layered model with a liquid layer on the top and a series of homogeneous isotropic solid layers, laying on a solid homogeneous isotropic half space (Fig. 1).

In such a simple situation, besides the reflected and refracted P waves, and the S waves in the solid layers, two other useful wave phenomena can be found. The first one corresponds to the interfacial waves propagating parallel to the water-sediment interface, with most of the energy concentrated at the solid-liquid interface, called Scholte waves (Scholte, 1958).

These waves are surface waves, and have an amplitude attenuation which is exponential with

the depth; they are dispersive, modal and hence similar to Rayleigh waves at the solid-air interface and to Stoneley waves at the solid-solid interface (Ewing *et al.*, 1957).

The second phenomenon corresponds to the guided waves associated to the leaking modes: in most of the common situation of shallow sediments, with a high Poisson ratio, these waves degenerate towards the simple modes of acoustic guided waves (Roth *et al.*, 1998). As the Scholte waves, they are dispersive, but they have a cut-off frequency which is quite high compared to the usual frequency ranges of conventional seismic prospecting. The phase velocity, higher than the Vp of the water at any frequency, depends on the compressional wave velocity of sediments.

In the following, the properties of the two wave phenomena are discussed and described referring to simple examples.

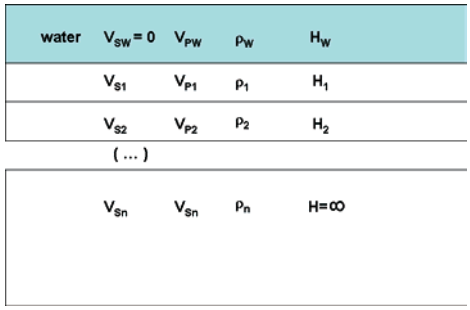

Fig. 1 - One-dimensional soil model for the Scholte wave propagation.

3. Scholte waves

Scholte waves are the normal modes, i.e. the eigenvalues related to real roots of the dispersion equation in the soft-bottom case, when the shear velocity of the solid is lower than the compressional velocity in the liquid (Carcione and Helle, 2004): they, hence, correspond to the Rayleigh solution at a solid-vacuum (air) interface. The particle motion of the Scholte waves is similar to those of the Rayleigh waves: given a sediment column, the Rayleigh velocity is, however, slightly higher than the corresponding Scholte velocity obtained when a water layer is present on the top. In the low frequency range, where because of the long wavelength the influence of water is reduced, the Scholte wave tends towards the Rayleigh wave in the solid sub-bottom sediments: in the high frequency range they tend towards the Stoneley wave at the solid-liquid interface. The velocity mainly depends on the shear wave velocity of the sediments, as in the case of the Rayleigh waves. The energy is concentrated at the interface, and attenuates rapidly when away from it: the penetration is roughly equal to one wavelength in the solid and to one wavelength in the liquid. High Scholte wave amplitude can be expected at the sea floor, where both the pressure field and the vertical component of the particle motion have their maxima. They can be excited by impact source at the interface or by pressure source in the water layer: according to Bohlen *et al*. (2004) a small airgun at the water surface can excite Scholte waves with sufficient amplitude for a water depth to 50 m.

Scholte waves are in general observed as low frequency and low velocity waves: the uppermost layer of the unconsolidated sediments can have a very low shear wave velocity [less than 50 m/s: Hamilton (1976), Aires and Theilen (1999)], and consequently, very low velocity Scholte waves are observed. In the following, the properties of the solution are shown referring to a simple three-layer model: two layers of thickness 2 m each and shear velocity of 150 m/s and 300 m/s and a half-space with a shear velocity of 600 m/s. The water layer is 2 m thick, and the

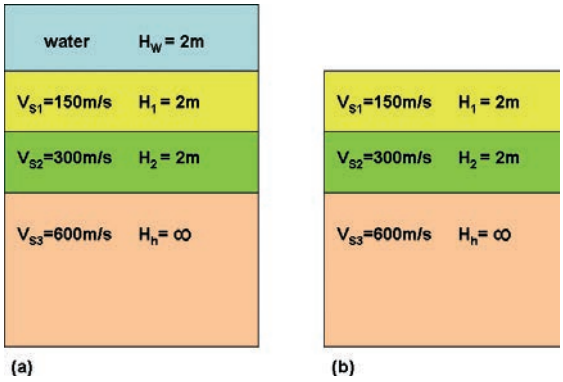

Fig. 2 - One-dimensional seismic model adopted with the major parameters for the simulation of the guided wave response with (a) and without (b) the water layer above the sediments.

P-wave velocities are respectively 1500 m/s, 1550 m/s 1600 m/s and 1800 m/s (Fig. 2a). The corresponding model used for the modelling and comparison of Rayleigh waves is depicted in Fig. 2b.

The solution is computed up to 100 Hz, and is compared to the corresponding Rayeigh wave solution, where the same elastic layers are not overlain by the water layer but by the vacuum. The dispersion curves of the two cases are depicted in Fig. 3: the fundamental mode and 4 higher modes are present in the considered

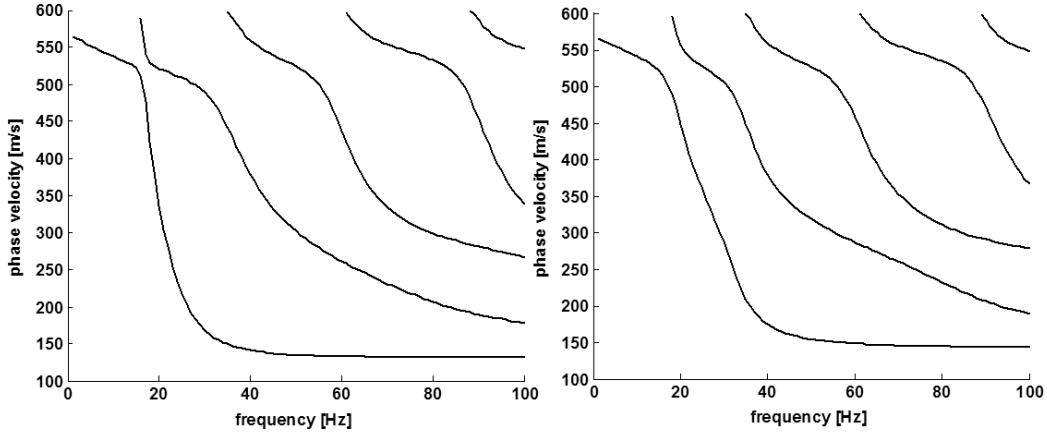

Fig. 3 - Modal curves of Scholte waves (left) and of Rayleigh waves (right) are compared to show the effect of the water layer on the phase velocities.

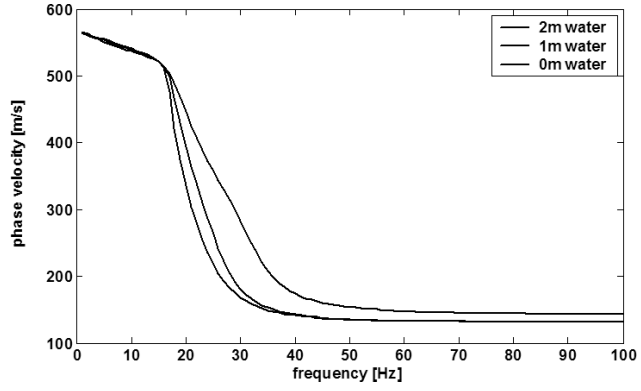

Fig. 4 - Rayleigh wave and Scholte wave first mode dispersion curve for the same layered system. The effect of the water is a reduction of the phase velocity in the high frequency range.

frequency range, and the effect of the water layer is a slight decrease of the phase velocity, particularly at high frequency.

The fundamental mode does not have a cut-off frequency, and at low frequency they tend towards the Rayleigh waves of the solid layered system. The difference of phase velocity, and the importance of modelling the water layer in the interpretation of Scholte wave data, is shown in Fig. 4, where the plot of the dispersion curves of the first normal mode is reported for a layered system with different thickness of the top water layer. The zero thickness case is of course the corresponding Rayleigh wave solution.

4. Leaking modes

The complex roots of the dispersion equation correspond to the leaking modes of propagation, with a phase velocity higher than the highest shear velocity in the system. The real part of the complex wavenumber corresponds to the acoustic propagation, and under some hypothesis, the imaginary part can be neglected: it has indeed been shown that, with a high Poisson ratio, the leaking modes can be approximated by the normal acoustic modes (Roth *et al.*, 1998; Roth and Holliger, 1999). This means that, when the Poisson ratio is higher than 0.4, this phenomenon is essentially composed of multiply reflected P-waves: it consists of compressional dispersive guided waves, whose phase velocity mainly depends on the P-wave velocity of the layers, which propagate with reduced attenuation. They are sometimes called ULF (ultra low frequency, in the range 1-100 Hz) in the domain of ocean acoustics: in the shallow applications, the frequency range can be centred to higher values. Considering a 2 m layer of sediments (Vp = 1560 m/s) above a bedrock (Vp = 2800 m/s), with a 2 m water depth, we compute the modal curves of the acoustic modes (Fig. 5): when observing the first mode, it is evident that the frequency range needed to estimate the velocities of the two solid layers is wide (from 100 to 1000 Hz).

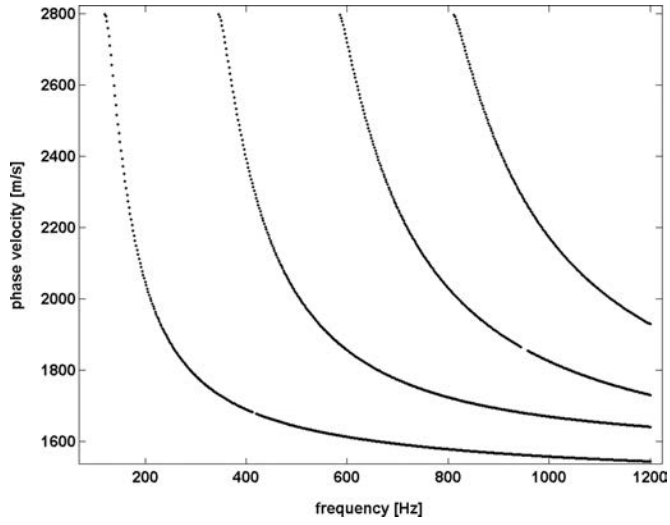

Fig. 5 - Dispersion curve of the acoustic modes for a simple two-layer model. The fundamental mode has a cut-off frequency of about 120 Hz.

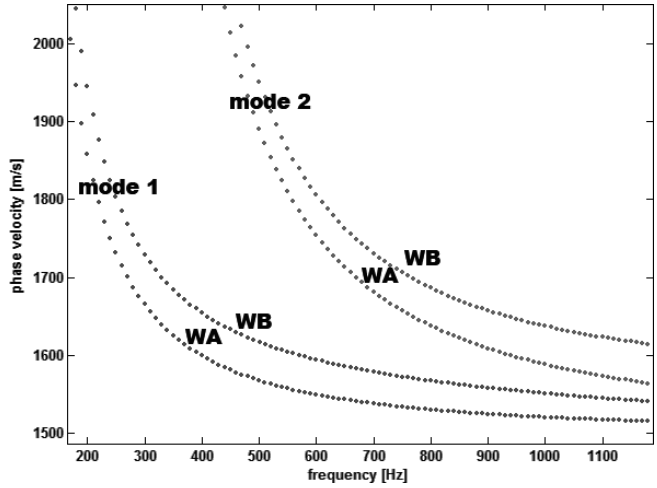

Fig. 6 - Effect of a small variation of the P-wave velocity (saturated unconsolidated sediments vs water) on the dispersion of the two first acoustic modes: WA 4 m of water with Vp = 1500 m/s, WB 2 m of water (Vp = 1500 m/s) and 2 m of sediments with Vp = 1570 m/s. The bedrock has Vp = 2800 m/s for both cases.

For the wavelengths greater than the layer thickness, the fundamental mode is dominating, while higher modes become important for shorter wavelengths. It can be noticed that the acoustic waves exist only above the cut-off frequency of the first mode. The case above the cut-off frequency of the fundamental mode is about 120 Hz, and in general, can be computed with a simple relation for a single-layer waveguide.

It is interesting to show how the presence of sediments influences the guided wave velocity, considering that the P-wave of unconsolidated sediments can be close to the P-wave of the water.

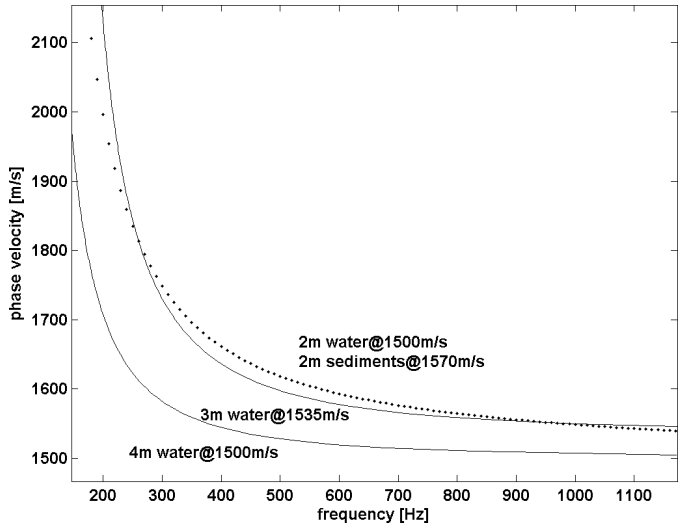

Fig. 7 - The two dispersion curves (fundamental mode) in Fig. 6 are compared to the dispersion curve of another one-layer model.

In the following example, a waveguide (WA) characterised by 4 m of water (Vp = 1500 m/s) over a half-space with Vp = 2800 m/s is compared to a waveguide (WB) with 2 m of water, then 2 of sediments with Vp = 1570 m/s: the first two acoustic modes are depicted in Fig. 6, where the increase of velocity of the two first modes due to the presence of the sediments is evident.

Clearly the phase velocity allows to discriminate between the two situations, if a wide frequency band is available: it is however worth remembering that the *a priori* information on the water thickness, in the case of very unconsolidated sediments, is very important for the inversion of such data. Fig. 7 shows the dispersion curve of a further model, with an intermediate water thickness and velocity, that can give a fairly good fitting to the real model. With a thin layer of soft sediments the *a priori* information on the water depth is hence of primary importance.

5. Acquisition

The two-wave phenomena can be used for a joint inversion to estimate the shear and compressional wave velocities that better constrain the geometrical parameters: a joint acquisition is possible if it allows a proper sampling, in time and space, of both the waves.

The two phenomena have two well separated ranges of frequency and velocity: Scholte waves propagate at a phase velocity close to the shear velocity of sediments, while guided waves propagate at a velocity higher than the compressional wave velocity in water. Moreover, the guided waves can have a cut off frequency higher than the upper limit of the Scholte wave frequency range of particular interest. In the case of Fig. 8 (2 m of water thickness, 1 m of sediments with Vp = 1560 m/s, 1 m with Vp = 1600 m/s, and bedrock with Vp = 2800 m/s) the cutoff frequency is about 120 Hz.

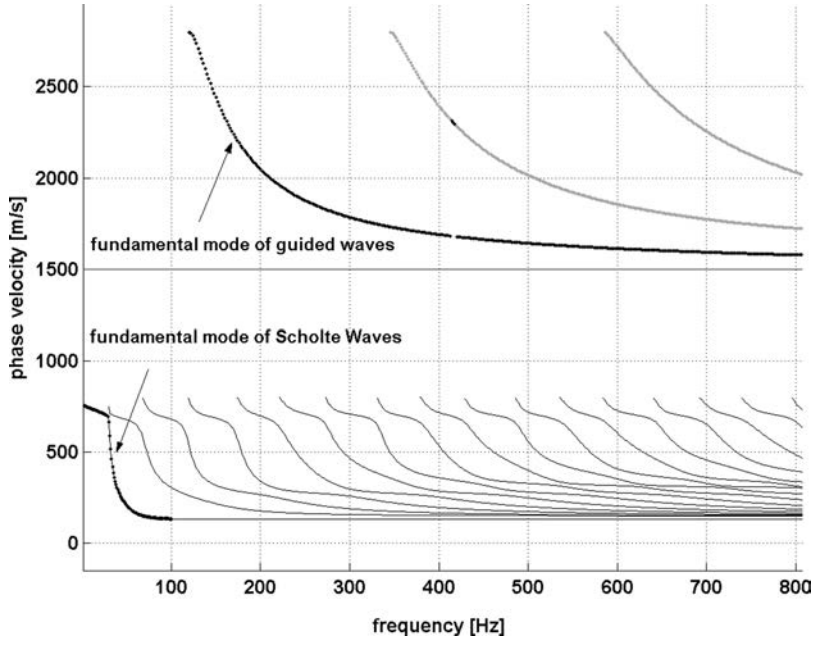

Fig. 8 - The dispersion curve of Scholte and guided waves plotted together shows the strong separation in velocity and in frequency for a shallow model.

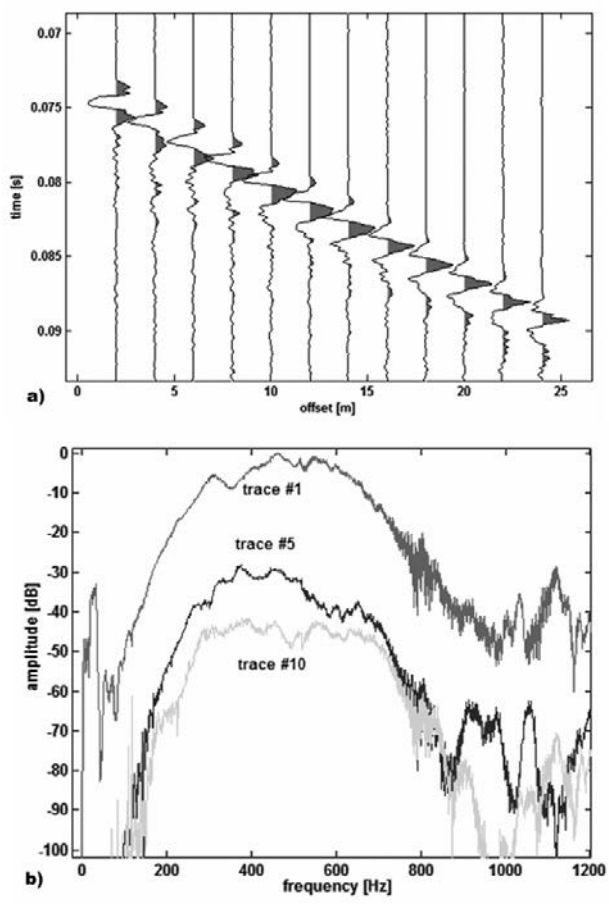

Fig. 9 - A shot gather is shown in a) and the frequency content of three traces is shown in b).

For all these reasons, these wavefields can be easily separated even though difficulties can arise because of the need for large ranges for the frequency and the wavenumber (the wavelength).

The acquisition of the two described wavefields can be performed recording the associated pressure field: the use of hydrophones at the sea bottom can effectively detect the pressure field related both to guided waves and to Scholte waves, and easily replace the acquisition of the vertical component of the particle velocity (Nicolas *et al.*, 2002).

A string of 12 hydrophones, with 2 m of spacing, has been proven effective for the analysis of the guided waves generated by a simple impulse source in water, a harpoon gun shot on a metal plate. The central frequency of the acquired traces is higher than 500 Hz, and the S/N is high in a wide frequency band (Fig. 9).

The wavelengths of the propagating waves, as better shown later on, range from 0.5 m to 30 m. The receiver spacing produces some spatial aliasing, which is however not critical: reducing the spacing would reduce the array length increasing the uncertainty on the long wavelength.

The shot gather, dominated by the high-frequency components related to guided waves, with a phase velocity greater than 1500 m/s, contains, however, also low-frequency and low-velocity phenomena, (10-40 Hz, phase velocity 80 m/s), which can be evidenced high-cut filtering the record. The presence of the two phenomena is much more evident in a raw record gathered across the shoreline (Fig. 10). The first 12 traces are gathered by 12 geophones on land, the other traces correspond to hydrophones on the sea bottom: the source (a sledgehammer) is located on the strand.

Even if the thickness of the water layer is gradually varying and some lateral effects (e.g. reflections) are present, the shot gather clearly identifies the presence of Rayleigh waves on land and of Scholte waves at sea: the 1D model could not be used for the inversion of these data. Considering the sea side of the array, it is evident, from the frequency range and the velocity range of the gathered waves, as well as the visual analysis, that both Scholte and guided waves have been recorded.

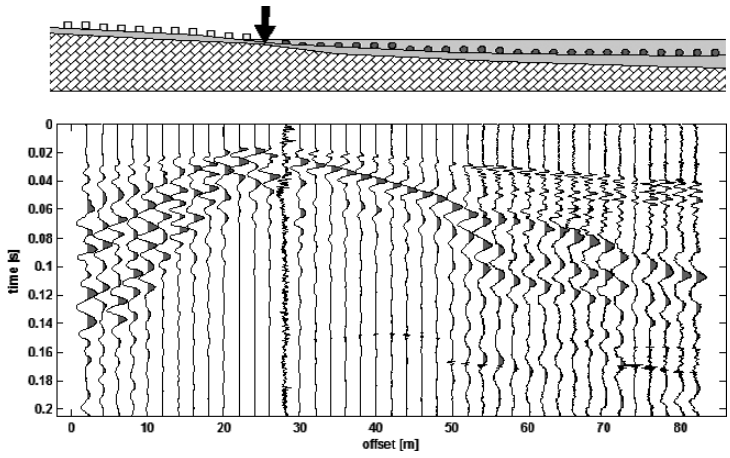

Fig. 10 - Scheme of the experimental set-up and corresponding shot gather. The shot position is on the strand, the first 12 traces are collected by geophones on land, while the others are collected by hydrophones placed on the sea bottom.

6. Processing and inversion

The data processing is based on the phase velocity analysis in the frequency domain, using the wavefield transform approach (McMechan and Yedlin, 1981): the velocity spectra allow the identification and separation of the different phenomena, and the estimate of the dispersion relation.

Records acquired for different shots with the same sensor array are analysed in frequency domain to evaluate the uncertainty; then data are averaged. The resulting shot gather is transformed from the time-offset domain into a frequency-wavenumber (f-k) domain, applying a 2D Fourier transform to obtain an f-k amplitude spectrum. In the f-k spectra the dispersive events are identified, and an automatic procedure search for the relative and absolute maxima at each frequency is performed. Some additional care must be taken to correct the spatial aliasing: the spectrum from the shot gather of Fig. 9, shows the presence of a dominant event in a wide-frequency range, with quite severe aliasing. The f-k spectrum of Fig. 11a is obtained by shifting the quadrant of the negative wavenumber (Socco and Strobbia, 2004) and normalising at each frequency: the continuity of an event in the whole frequency range is evident, as is the spatial aliasing that wraps the maximum in the range [0-pi] rad/s (Fig. 11b); in this case, the aliasing is easily corrected, and a dispersion curve can be obtained in a large bandwidth (Fig. 11c).

The search for the maxima position allows the identification of the phase velocity-frequency relation (dispersion curve) corresponding to the guided waves. The curve depicted in Fig. 11a shows a fundamental mode and some branches of higher modes.

The dispersion curve has to be inverted to identify the corresponding layer model: the parameterisation of the model is a crucial point (as in the inversion of the MASW – Multichannel Analysis of Surface Waves) for the reliability of the result. In this case, the simplest 3-layer model can be assumed: liquid layer, sediments, and bedrock (Ewing *et al.*, 1957). The sensitivity is

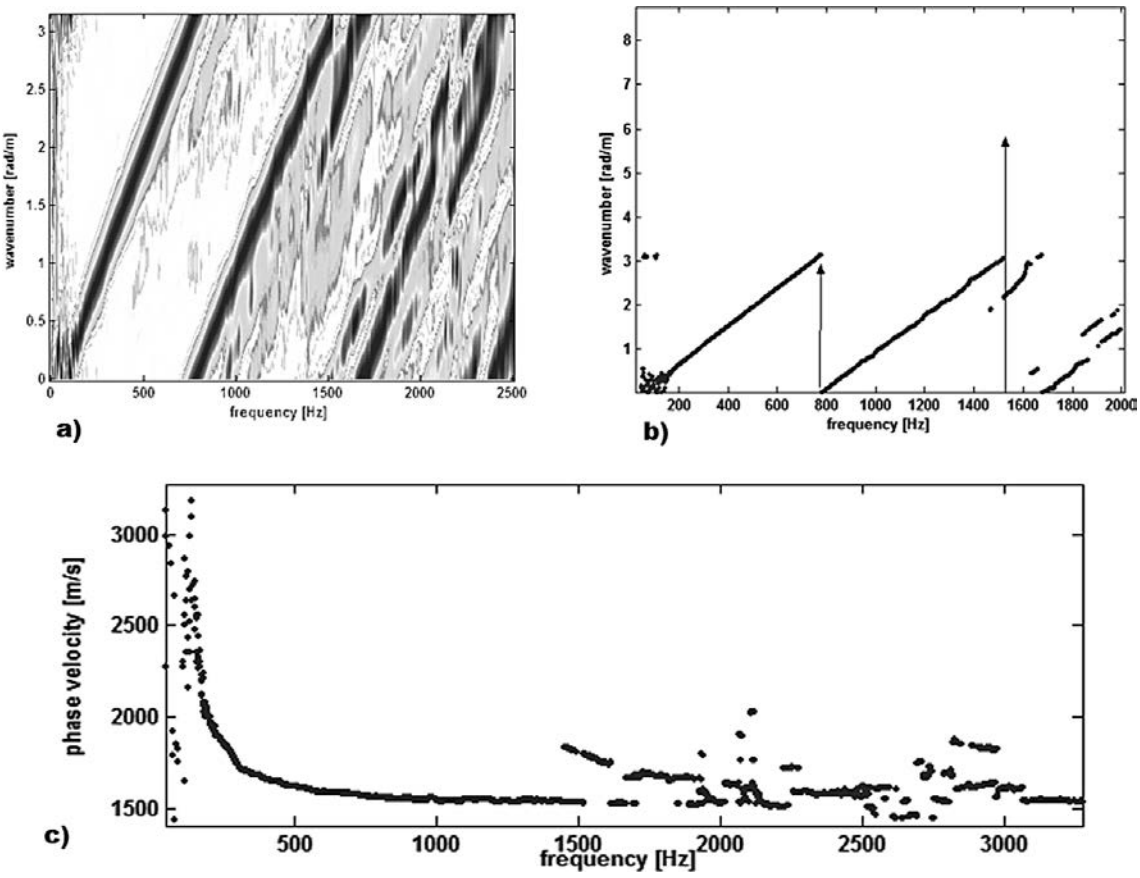

Fig. 11 - Processing of the shot gather in Fig. 9. The f-k spectrum (a) with multiple spatial aliasing, (b) the f-k position of maxima to be unwrapped, and (c) the final dispersion curve.

controlled by P-wave velocity, and hence, the inversion is performed for the P-wave velocity of the three media.

The Scholte wave dispersion curve, on the other hand, is inverted to determine the shear wave velocities of the sediments and the bedrock. The Scholte wave dispersion curve is obtained using the same approach, after low-pass filtering the shot gather to enhance and check the presence of the coherent event: the dispersion curve is depicted in the following Fig. 12, where the low frequency and velocity ranges are to be noticed.

If the data quality is high and the model parameterisation is correct, the influence on the result of the chosen inversion algorithm is poor. Several approaches have been proposed for the one-dimensional inversion, belonging both to local and global search. Considering the inversion step of the method, it can be said that there is no big difference with respect to the onshore surface-wave method.

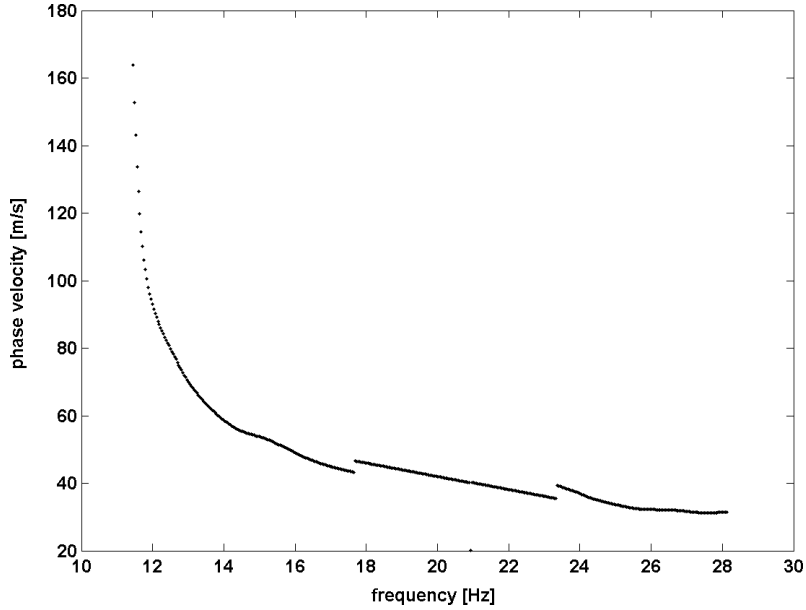

Fig. 12 - Dispersion curve of Scholte waves extracted from the shot gather in Fig. 9.

A first model is generated automatically on the basis of the phase velocity and the wavelength, then an iterative damped least-square optimisation with few iterations gives the final model. The sensitivity to the thickness parameter is shown in Fig. 13, where the curve of the best fitting model is shown together with two other curves corresponding to different values of thickness of sediments.

Even if the joint interpretation of different geophysical tests can also be used to increase the reliability of the results, the joint or mutually constrained inversion is a more robust tool to infer a final model, using the information about different phenomena and physical parameters. This allows the reduction of the ambiguities due to the non-uniqueness of the inverse problem solution (Tikonov and Goncharsky, 1987). This approach has been adopted in mixing seismic and electric data (Hering *et al.*, 1995; Misiek *et al.* 1997) and in joining the information of Rayleigh and guided waves (Roth *et al.*, 1998).

The joint inversion of Scholte waves and guided waves is a natural approach: the coupling of the two models via the geometrical parameters (thickness of the layers) is easily implemented. A single data kernel can be implemented in a linearised approach, building a single Jacobian matrix. Considering the data ($V_{Scholte}$ and V_{Guided}) and the model parameter (V_S, V_P and H), the non-zero derivatives of both the Scholte and guided waves with respect to the layer thicknesses produce the coupling, even if the derivatives of the Scholte waves with respect to the Vp and of the guided waves with respect to the Vs, are zero.

A further improvement could be the introduction of electric data in the joint inversion: the geometry, however, should be consistent and hence one-dimensional (Hering *et al*., 1995).

In the present case, the electric data are a multielectrode ERT, and a 2D model is used for the inversion: the results are hence used for comparison, and for a joint interpretation of the physical parameters of the sediments.

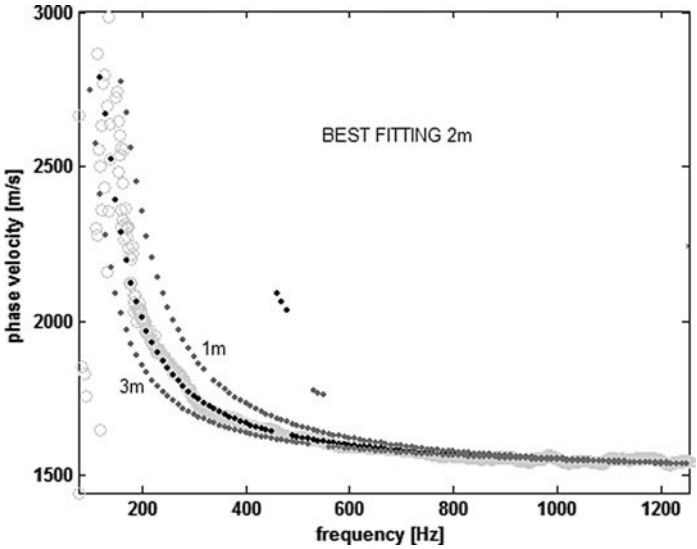

Fig. 13 - The best-fitting curve for the guided waves (corresponding to a model with a sediment thickness of 2 m) is shown together with two other curves for two different values of the parameter.

7. Comparison to other data

We checked the possibility of integrating seismic data with electrical data for marine sediments in shallow water, where characterisation of geotechnical properties is required. In situ measurements of electrical resistivity offer a cost and time effective method for obtaining a comprehensive overview of near surface, sediment physical properties, such as porosity and sediment thickness. They also provide a quality check for in situ measurements of related sediment properties or for data obtained from sediment core analysis: Jansen *et al.* (2005) describe some results obtained by means of a sediment-penetrating, in situ probe which logs electrical resistivity of marine sediments.

The adopted technique is the 2D electrical resistivity tomography. The resistivity data were collected with Syscal Resistivity Meter R1 with dipole-dipole and Wenner-Schlumberger electrodes array; 24 small electrodes were placed on the sea bottom at 2 meter intervals. The data were inverted using RES2DINV software which allows one to take into account the effect of the sea water above the electrodes and of the sea-bottom topography. The inversion process has been constrained by taking into account the water resistivity and the theoretical range of values of the resistivity of the sediments.

In order to assess the effectiveness of the use of in situ resistivity data for the characterisation, we discuss the relationships between the petrophysical parameters, such as the porosity, and the resistivity for saturated unconsolidated sediments. The bulk resistivity of fully saturated sediments ρ is a function of water resistivity ρ_w, porosity ϕ and texture, and usually the ratio ρ/ρ_w is called formation factor F.

The resistivity of pore-water is mainly a function of the temperature and the dissolved salt content (salinity) of the pore water. Pore-water salinity is available from the analysis of interstitial water samples. In general, the interstitial water salinities near the sediment-water interface is about 35 ppt. The formation factor is empirically related to the porosity by several equations

(Archie, 1942; Atkins and Smith, 1961; Bear, 1972). From literature, the porosity formation factor relationship states that for clean sand

$$F = \frac{a}{\phi^m}$$

where F stands for the formation factor and a (close to 1) and m represent empirical constants that depend on the sediment characteristics (e.g., Iversen and Jørgensen, 1993).

Experimental studies on real marine sediments found other relationships: for example, on deep-sea Tyrrhenian sediments a good fit with experimental data in the high porosity range (0.5-0.8) is given by polynomial relationships (Kermabon *et al.*, 1969).

On the other hand, theoretical studies considering more complex textures developed relationships starting from Archie's law, and including mixtures of two-shaped particle types (Jackson *et al*., 1978). The relationship may be applicable to marine sediments in general, being in agreement with published data for marine clays. The exponent m depends on the shape of the particles and it increases as they become less spherical, varying from 1.2 for spheres to 1.9 for platey shell fragments. These results were validated in the porosity ranging from 0.3-0.5.

These considerations allow the definition of boundaries for the resistivity of shallow, saturated, unconsolidated sediments. In particular, a raw estimate of sediment porosity (in the range between 0.4-0.5), and the measurements of the sea-water resistivity permit us to compute upper and lower limits for the bulk sediment resistivity.

The upper (for bedrock) and the lower (for high-porosity sediments) limits that can be adopted to constrain the resistivity in the inversion process are summarised in Table 1

A simplified sensitivity analysis has been performed, inverting 2D synthetic data sets, in order to evaluate the effectiveness of the ERT in estimating the thickness of the sediments embedded between marine water and calcareous bedrock. The resistivity values of sediments and bedrock has been estimated according to the Archie law and the parameters reported in Table 1, for an average porosity of 0.5.

The resistivity model of Fig. 14 refers to sediments with a 2-meter thickness and resistivity of 0.6 ohm·m overlying a bedrock with resistivity equal to 50 ohm·m. The pseudosection shows a

Table 1 - Estimate of formation factor and resistivity values for the saturated sediments and bedrock.

Sediments	Porosity	Cementation factor (*m*)	Ref.	Formation factor (*F*)	Resistivity [ohm·m]
sphere	0.30	1.2	J	4.24	1.1
	0.40	1.2	J	3.00	0.8
	0.50	1.2	J	2.30	0.6
platy shell	0.30	1.9	J	9.85	2.5
	0.40	1.9	J	5.70	1.4
	0.50	1.9	J	3.73	0.9
calcareous bedrock	0.05	1.9	S	296.45	74.1
	0.10	1.9	S	79.43	19.9
Fluid					0.2

J - Jackson *et al.* (1978).
S - Schön (1996).

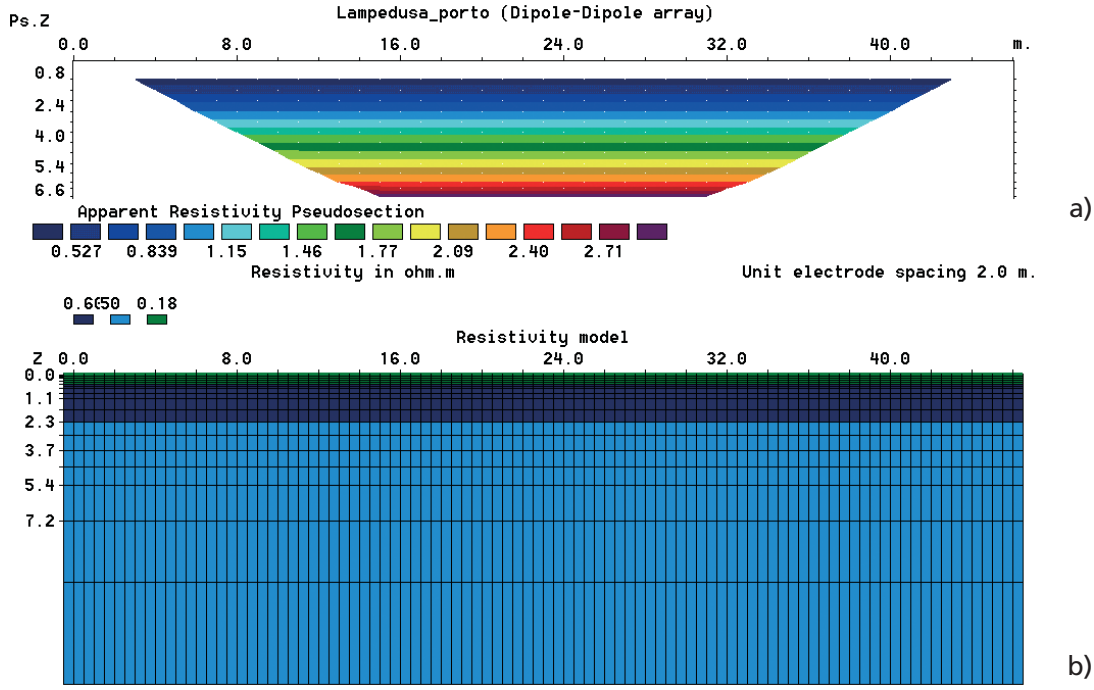

Fig. 14 - Resistivity modelling. a) Apparent resistivity pseudosection. b) Two-layer model used to compute the synthetic pseudosection: the upper layer, 2 m thick with resistivity equal to 0.6 ohm · m represents the saturated sediments and the lower layer (50 ohm · m) represents the bedrock.

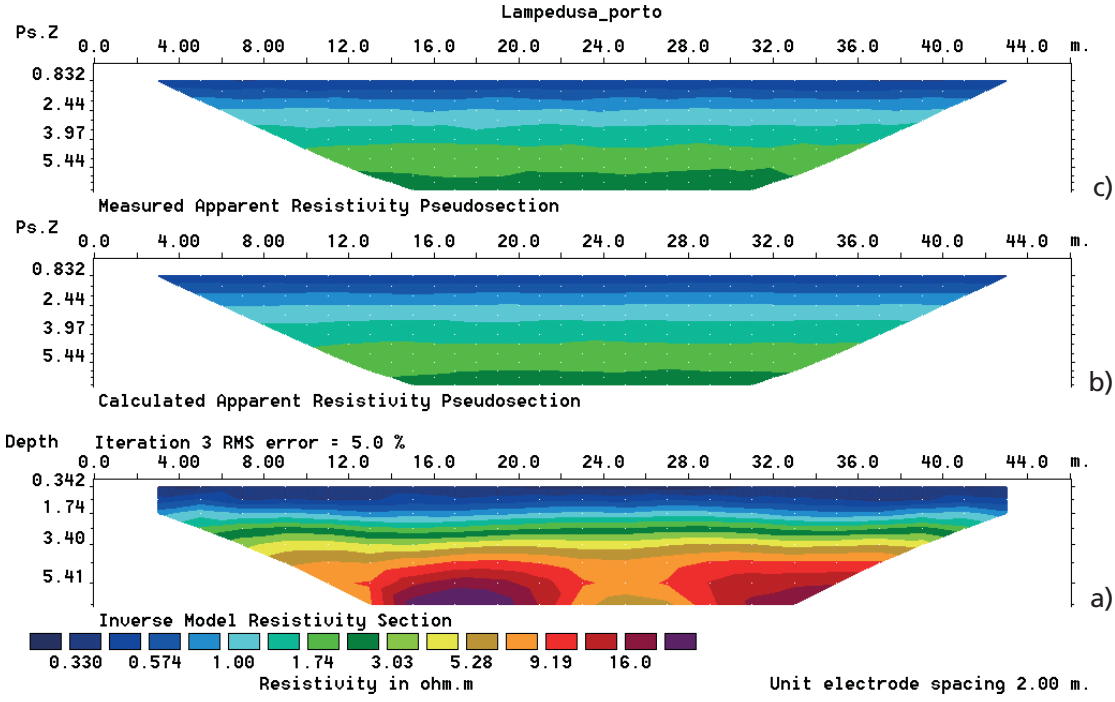

Fig. 15 - a) Resistivity model after the inversion of the synthetic data set plotted in Fig. 14; b) calculated apparent resistivity pseudosection; c) apparent resistivity pseudosection simulated on the model in Fig. 14.

gradual increase of the apparent resistivity with depth, ranging from about 0.6 ohm·m up to 3 ohm·m. The subsequent inversion of the apparent resistivity data set (adding a random noise of 5%) is depicted in Fig. 15; resistivity values range from 0.33 ohm·m to 16 ohm·m, showing an underestimation of the effective resistivity values of sediments and bedrock. With a certain ambiguity the inversion process permits a rough estimate of the sediment thickness, considering the abrupt resistivity gradients that can be detected at a depth of 2 m. These uncertainties are mainly linked to the limits in vertical resolution of the dipole-dipole configuration array; the improvement of the vertical resolution adopting an hybrid array, such as the Wenner-Schlumberger array, does not appear so effective, using only 24 electrodes.

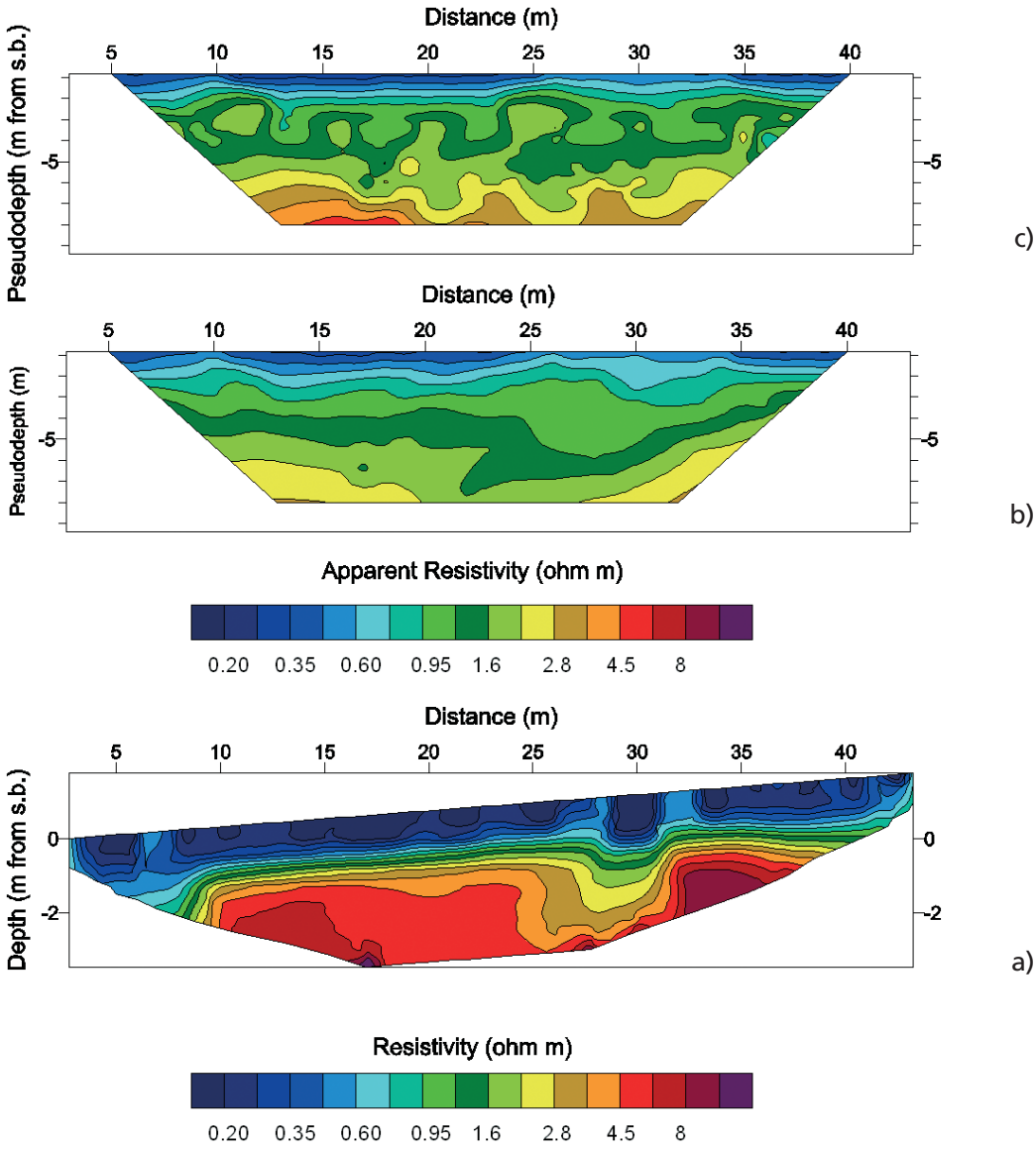

Fig. 16 - Result of the inversion on experimental data for test site 1 using 24 electrodes on the seabottom in a dipole-dipole configuration array. a) final resistivity model; b) computed apparent resistivity pseudosection: c) experimental data pseudosection. Depth is measured in meters from the sea bottom.

Some experimental results are depicted in Figs. 16 and 17; in the first test site, the results of the robust inversion permit us to estimate the thickness sediments ranging between 2-2.5 m; sediments are characterised by resistivity values of about 0.3 ohm·m, corresponding to a porosity value equal to 0.8, according to the Archie law, with a m = 1.9 and a = 1 cementation factor.

In the second site (Fig. 17), resistivity values ranging from 0.3 ohm·m to 0.4 ohm·m indicate the response of the marine sediments, moreover, the calcareous bedrock is characterised by values

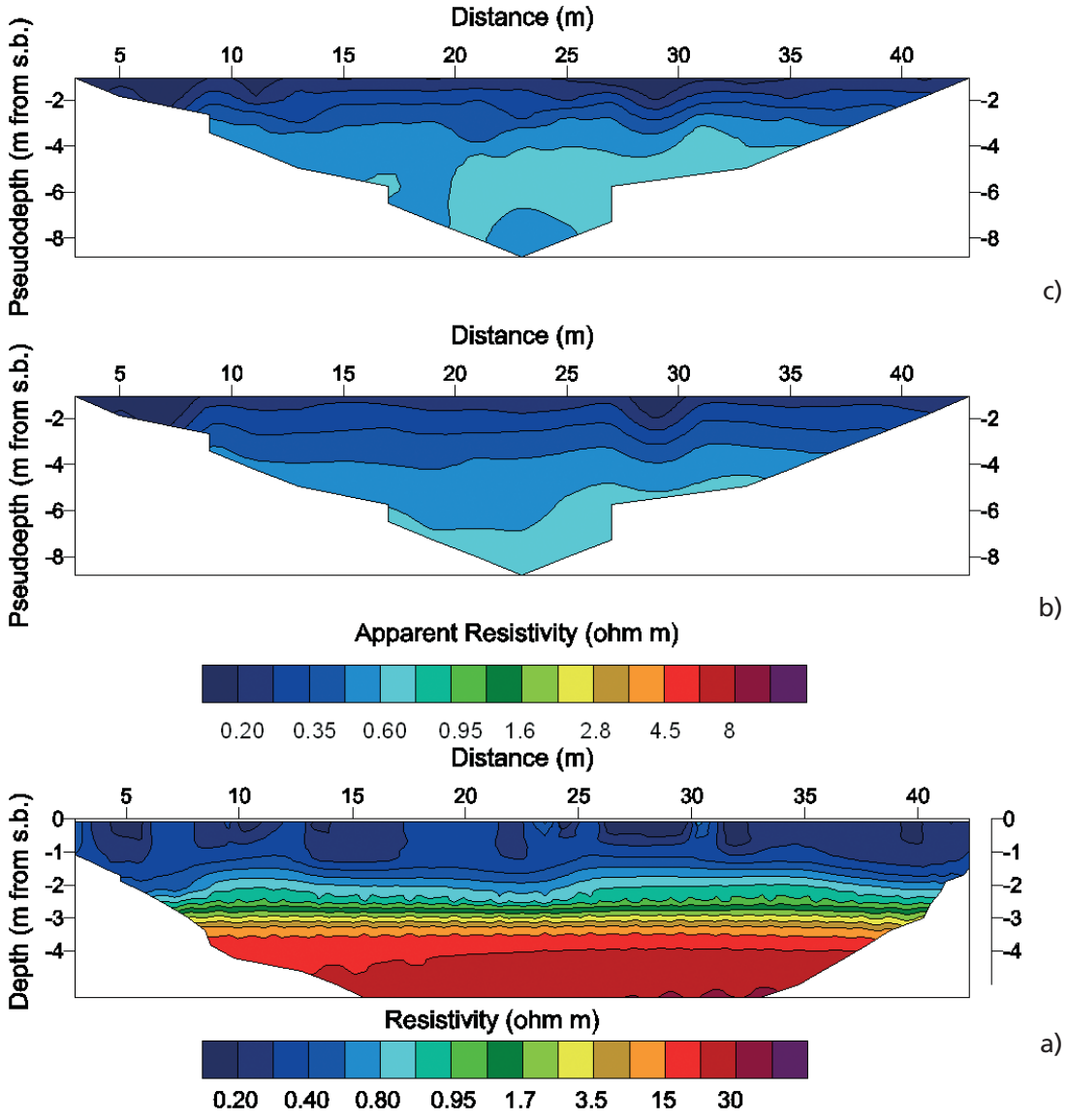

Fig. 17 - Result of the inversion on experimental data for test site 2 using 24 electrodes on the sea bottom in a dipole-dipole configuration array. a) Final resistivity model; b) computed apparent resistivity pseudosection: c) experimental data pseudosection. Depth is measured in meters from the sea bottom.

ranging from 5 ohm·m to 30 ohm·m. The porosity values of sediments are estimated in the range between 0.7 and 0.8 (m = 1.9, a = 1). This rough estimate of porosity does not take into account the uncertainty in the determination of actual resistivity value of the sediments as pointed out by the consideration on synthetic data.

The acquisition with a conventional resistivity meter can, however, give some problems because of the very high conductivity: an accurate control of the input is needed to prevent the damage due to a high current, and special materials are needed to prevent oxidation.

8. Conclusions

Experimental evidence of guided waves and Scholte waves are present in data acquired using simple hydrophones on the sea-bottom in shallow water; joint analysis of these two phenomena permits us to determine the thickness of saturated porous sediments embedded between sea water and hard bedrock. Because of the high porosity (over the critical porosity limit) and the low compaction of the shallow sediments, the P-wave velocity is dominated by the fluid compressibility much more than by the compressibility of the solid skeleton and, therefore, the use of this wavefield is not diagnostic of sediment properties. The situation of a thin layer of soft sediments can be particularly difficult: the bedrock-sediments impedance contrast can be very high for shear properties, and the water-sediment contrast can be very low for compressional properties.

Ambiguities in seismic data processing of guided and Scholte waves could be avoided or reduced using resistivity data acquired with sea-bottom electrodes: the interpretation of resistivity data permit us to estimate the range of values for the sediment layer that must be adopted in the dispersion curve analysis.

The reliability of using resistivity data for fixing constraints in the inversion process of Scholte and guided waves is acceptable for a reduced thickness of sediments; on the other hand a direct calibration of the porosity or punctual resistivity measurements within the sediments would increase the reliability of the ERT porosity estimate.

Moreover, much experimental effort must be made in view of an useful adoption of the suggested procedure to estimate spatial variability of the mechanical properties (porosity) of sediments.

REFERENCES

Ayres A. and Theilen F.; 1999: *Relationship between P- and S-wave velocities and geological properties of near-surface sediments of the continental slope of the Barents sea*. Geophysical Prospecting, **47**, 431-441.

Archie G.E.; 1942: *Electrical resistivity log as an aid in determining reservoir characteristics*. Trans. Am. Inst. Min. Metall. Petrol. Eng., **146,** 54-62.

Atkins E.R.J. and Smith G.H.; 1961: *The significance of particle shape in formation resistivity factor-porosity relationships*. J. Petrol.Technol., **13,** 285-291.

Bear J.; 1972: *Dynamics of fluids in porous media*. Elsevier, Amsterdam, 764 pp.

Bohlen T., Kugler S., Klein G. and Theilen F.; 2004: *1.5D inversion of lateral variation of Scholte-wave dispersion*. Geophysics, **69**, 330-344.

Caiti A., Akal T. and Stoll R.D.; 1994: *Estimation of shear wave velocity in shallow marine sediments*. IEE Journal of Oceanic Engineering, **19**, 58-72.

Carcione J.M. and Helle H.B.; 2004: *The physics and simulation of wave propagation at the ocean bottom*. Geophysics, **69**, 825-839.

Deidda G.P. and Balia R.; 2001: *An ultrashallow SH-wave seismic reflection experiment on a subsurface ground model*. Geophysics **66**, 1096-1104.

Ewing W.M., Jardetzky W.S. and Press F.; 1957: *Elastic waves in layered media*. McGraw-Hill, New York, 380 pp.

Hamilton E.; 1976: *Shear wave velocity versus depth in marine sediments: a review*. Geophysics, **41**, 986-996.

Hering A., Misiek R., Gyulai A., Ormos T., Dobroka M. and Dresen L.; 1995: *A joint inversion algorithm to process geoelectric and surface wave seismic data. Part I: basic ideas.* Geophysical Prospecting, **43**, 135-156.

Kermabon A., Gehin C. and Blavier P.; 1969: *A deep-sea electrical resistivity probe for measuring porosity and density of unconsolidated sediments*. Geophysics, **34,** 554-571.

Iversen N. and Jørgensen B.B.; 1993: *Diffusion coefficients of sulfate and methane in marine sediments: influence of porosity*. Geochim. Cosmochim. Acta, **57,** 571-578.

Jackson P.D., Smith, D.T. and Stanford P.N.; 1978: *Resistivity-porosity-particle shape relationships for marine sands*. Geophysics, **43,** 1250-1276.

Jansen D., Heesemann B., Pfender M., Rosenberger A. and Villinger H.; 2005: *In situ measurement of electrical resistivity of marine sediments, results from Cascadia Basin off Vancouver Island.* Marine Geology, **216**, 17-26.

McMechan G.A. and Yedlin M.J.; 1981: *Analysis of dispersive waves by wave field transformation*. Geophysics, **46**, 869-874.

Misiek R., Liebig A., Gyulai A., Ormos T., Dobroka M. and Dresen L.; 1997: *A joint inversion algorithm to process geoelectric and surface wave sismic data. Part II: applications.* Geophysical Prospecting, **45**, 65-85.

Nicolas B., Mars J., Lacoume J.L. and Fattaccioli D.; 2002: *Are ultra low frequency waves suitable for detection?* IEEE/MTS Oceans02, Biloxi, 1109-1113.

Roth M. and Holliger K.; 1999: *Inversion of source-generated noise in high-resolution seismic data*. The Leading Edge, **18**,1402-1406.

Roth M., Holliger K. and Green A.G.; 1998: *Guided waves in near-surface seismic surveys*. Geophysical Research Letters, **25**, 1071-1074.

Scholte J.G.J.; 1958: *Rayleigh wave in isotropic and anisotropic elastic media*. Meded. en Verhand. KNMI, **72**, 9-43.

Schon J.H.; 1996: *Physical properties of rocks: fundamentals and principles of petrophysics*. Handbook of Geophysical Exploration, Seismic Exploration, vol. **18**. Pergamon Press, 583 pp.

Shtivelman V.; 2001: S*hallow water seismic surveys for the site investigation in the Haifa Port Extension area, Israel.* Journal of Applied Geophysics, **46**, 143-158.

Shtivelman V.; 2004: *Estimating seismic velocities below the sea-bed using surface waves*. Near Surface Geophysics, **2**, 241-247.

Socco L.V. and Strobbia C.; 2004: *Surface wave method for the near surface characterisation: a tutorial*. Near Surface Geophysics, **4**, 165-185.

Stoll R.D. and Bautista E.; 1994: *New tool for studying seafloor geotechnical and geoacousical properties*. Journal of the Acoustical Society of America, **96**, 2937-2944.

Tikonov A.N. and Goncharsky A.V. (eds).; 1987: *Ill-posed problems in the natural sciences.* MIR Publishers, Moscow.

Winsborrow G., Huws D.G. and Muyzert E.; 2003: *Acquisition and inversion of Love wave data to measure the lateral variability of geoacoustic properties of marine sediments*. Journal of Applied Geophysics, **54**, 71-84.

Corresponding author: Claudio Strobbia
EUCENTRE - European Centre for Training and Research on Earthquake Engineering
c/o Università di Pavia, Dip. Mecc. Strutt.
Via Ferrata 1, 27100 Pavia, Italy
phone: +39 0382 516925; fax: +39 0382 529131; e-mail: claudio.strobbia@eucentre.it